Proceedings of the 2026 Design of Medical Devices Conference
DMD2026
April 20-22, 2026, Minneapolis, MN, USA

DMD2026-1076

ESTIMATING THE NON-PARAMETRIC JACOBIAN OF A TENDON-DRIVEN SOFT ROBOT END-EFFECTOR

Orla Gotthelf, PhD
University of Minnesota
Minneapolis, MN

Yusra Farhat Ullah, PhD
University of Minnesota
Minneapolis, MN

Ronak Narkhede
University of Minnesota
Minneapolis, MN

Timothy M. Kowalewski, PhD
University of Minnesota
Minneapolis, MN

ABSTRACT

Soft robots have the potential to navigate tortuous pathways such as those found in human anatomy owing to their compliant nature and low risk of injury to soft tissues. However, their control is challenging due to the lack of reliable closed-form analytical models. Recently, kinematic-free control has been used to bypass analytical modeling. While online Jacobian estimation has been explored in various soft robot configurations, it has not been demonstrated in three-cable driven soft arms without backbones, particularly using computer vision and electromagnetic tracking for workspace exploration. This study addresses this gap by implementing online Jacobian estimation through workspace exploration in a three-cable driven soft arm through visual servoing and integrating an Ascension trakSTAR system for occlusion-free position feedback.

Keywords: Soft Robotics, Jacobian Estimation, Model-free Control, Electromagnetic Tracking, Visual Servoing

NOMENCLATURE

EMTS	electromagnetic tracker-based servoing
IBVS	image-based visual servoing

1. INTRODUCTION

Soft robotics can provide treatment options for no-option patients (i.e. patients with tortuous vascular anatomy) due to the ability of the soft body to conform to varying anatomy. To add to the complexity, the anatomical pathways such as vascular system or bronchial system contain a multitude of branching points or bifurcations and trifurcations that a robot needs to navigate. Presently available rigid and semi-rigid hyper-redundant manipulators can track arbitrary paths, but their rigid nature requires a certain degree of care, and sensory feedback, in a system as delicate as human anatomy to avoid damage. The compliant nature of soft robots is ideally suited to this task, but their control is made challenging due to the lack of a reliable analytical model. The modeling of soft robots is challenging due to their highly non-linear nature and the involvement of infinite degrees of freedom.

Prior work in the field has approached the approximate analytical kinematic and dynamic modeling of continuum robots in multiple ways, which are listed comprehensively in [1]. These approximations are based on heavy simplification and require increasingly higher computation power for increasing complexity. Furthermore, unknown environmental factors can result in an inaccurate analytical model approximation.

Model-less or kinematic-free control has been used to control the position of a robot without using an explicit closed-form analytical model. EnRoco, a 2-DOF planar robot was the first robot to use a learning-based encoder-less control [2]. EnRoco uses camera tracking to learn a robot model based on actuation, instead of joint velocities, required to achieve a commanded movement. The learned robot model is stored in long-term memory. Li et al. [3] proposed a position controller for a home service robot with a deformable manipulator that generates control signals (actuation) by solving the pseudo-inverse of estimated Jacobian without learning algorithm or optimization. In another work [4], Li et al. estimated the Jacobian through incremental actuation and end effector measurement. Segments of a geodesic of SO(3) from current orientation to target orientation are used to map orientation to actuation locally. However, Li et al.'s work deals only with predicting orientation. Another study uses a Feed-forward Neural Network to learn the global controller for planar movement in a 3-cable driven soft arm [5], however, it relies on an approximate analytical model to initiate learning.

Wang et al. [6] experimentally demonstrated that model-free control achieves higher accuracy than model-based control in robotic catheters. Yip and Camarillo [7] showed that a position control law based on online model-free Jacobian estimation can overcome artificial singularities that would otherwise arise from environmental constraints in model-based Jacobian approaches. This position controller was later extended to a hybrid position-force controller [8], where the Jacobian is estimated online using both position and force feedback. Lee, et al. implemented model-free feedback in a hydraulically actuated 3-chamber soft arm for endoscopy [9] using a Finite Element Model to initialize the control loop, followed by Jacobian estimation via Locally Weighted Projection Regression during subsequent actuation.

While the aforementioned studies are not exhaustive, none addresses online Jacobian estimation in a three-cable driven soft arm without a backbone. This research aims to fill this gap by evaluating the accuracy of online Jacobian estimation for mapping tip position from 2D task-space to 3D joint-space through workspace exploration. This approach could enable directional control of soft robots navigating unknown, confined environments such as human anatomy. By conceptualizing a soft robot as two distinct systems—an end effector and a locomotion system—the end effector can serve as a decision-making unit that guides the locomotor component. For example, in the navigation of tortuous pathways in the human body a catheter would be providing the 3rd dimension of movement as it is pushed and pulled through the vasculature with the end effector directing navigation at branching points.

Two approaches were chosen: end-point open loop (or eye-to-hand) image-based visual servoing (IBVS) and electromagnetic tracker-based servoing (EMTS). In IBVS the control signal is based on the difference between the observed image features and the desired image features where as EMTS control signals are generated from the difference between measured end effector coordinates and target positions. The specific research aims are to: (1) design and construct a three-cable driven soft arm capable of both IBVS and EMTS, (2) estimate the numerical Jacobian mapping between end effector positions and cable actuation, and (3) implement the Jacobian estimation algorithm to achieve desired end effector positions.

2. MATERIALS AND METHODS

2.1 Manufacturing of the End Effector

The cable driven soft robot end effector is comprised of a semi-hollow cylindrical chamber, connected to three actuation cables located at equidistant points around its front end. Two variations of cable placement were used: one with the cables attached externally, and the other with the cables embedded within the body of the robot to better represent a more realistic version of a catheter. Both soft end effectors are made of Poly 74 Series polyurethane from Polytech, have an outer diameter of 13mm and an inner diameter of 4mm while being 90-mm long.

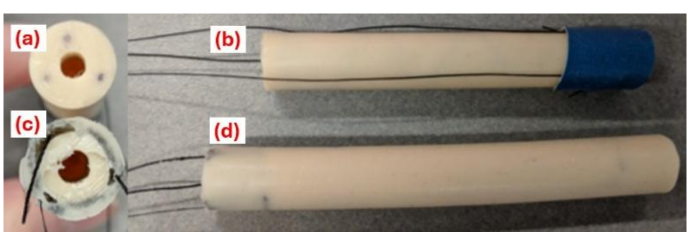

FIGURE 1: (a) Bottom view of external cable soft body, black dots are from a marker, (b) Side view of external cable soft body, (c) Bottom view of embedded cable body showing cables exiting the body, (d) Side view of embedded cable body

The fabrication process of the robot is dependent on the location of the cables. External cables robots are created in two steps: casting followed by cable attachment. However, embedded cables require a three-phase manufacturing process: casting, cable attachment and reinforcement, and recasting. The embedded cables are coated with Vaseline below the attachment site to prevent the cables from binding with the polyurethane during the recasting. Fabric reinforcement is achieved by gluing a ring of fabric around the bottom of the robot with three connection sites offset to be in the middle of the spaces between the cable attachments. This serves two purposes: make sure the cables stay straight by restricting lateral movement of the cables and to prevent the cable from cutting through the soft polyurethane when pulled upon. The polyurethane robot is cast by a 3D printed mold that is inserted into a stainless-steel tube - both coated by a Teflon non-stick spray. The material is placed into a vacuum chamber to remove all air bubbles and is injected from the bottom of the cast to resist air pockets from forming during the casting process. The finished product of both robot types can be seen in Figure 1.

The cables extending out from the soft arm are actuated by three HiTec servo motors, which are controlled by an Arduino Uno. The Arduino Uno holds serial communication with the main Python program to receive the next servo position and send current servo position.

The soft arm is mounted in a 3D-printed holder assembled to the acrylic housing containing the servos, the Arduino, and a circuit board. Figure 2 shows the simple schematic used for controlling the robot and Figure 3 shows the front and back of the assembled device.

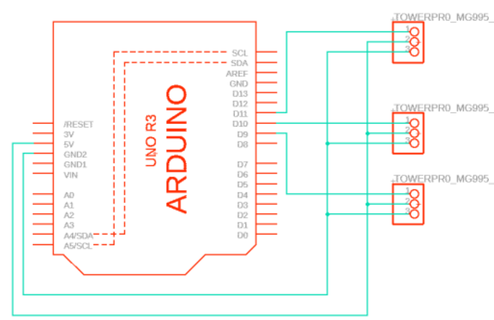

FIGURE 2: Arduino Schematic

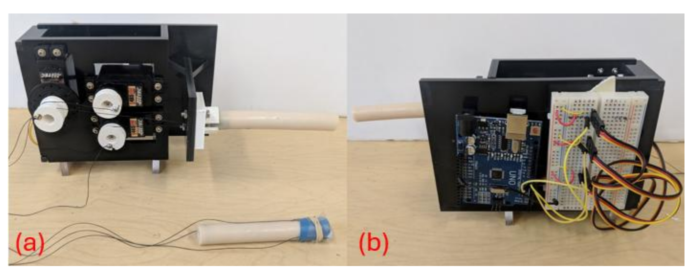

FIGURE 3: (a) Assembled soft robot end effector showing connection to servo drive system. Attached to the robot is the soft body with internal actuators, unattached to the robot is the soft body with external actuators. (b) The Arduino and circuitry that drive the robot

2.2 Computer Vision and Electromagnetic Tracking

IBVS implemented using a webcam, an ArUco marker, and OpenCV in Python 2.7. OpenCV can track the center point of the ArUco marker, a 2D image not dissimilar from a QR code, to determine the location of the end effector. IBVS exists all in 2DOF and uses a subset of a 2D task-space known as pixel-space where measurements are taken in pixels.

EMTS was additionally selected for position feedback as vision-based systems are impractical in scenarios such as navigation within human anatomy, where optical occlusion and limited visibility prevent reliable tracking. The EMTS was implemented using an Ascension trakSTAR system, comprising a desktop electronics unit paired with a Mid-Range Transmitter (MRT) and a Model 130 6DOF electromagnetic sensor as shown in Figure 4. The EMTS data is transmitted via serial using Python 3. The task-space for EMTS is measured in millimeters.

The Model 130 sensor's maximum outer diameter of 1.5 mm enables it to be embedded within the semi-hollow cylindrical chamber of the end effector shown in Figure 5, providing real-time position and orientation data without requiring line-of-sight. The Model 130 has user-configurable update rate from 20-255Hz. The static accuracy for position is1.4mm RMS and for orientation is 0.5° RMS. The MRT allows tracking of the Model 130 within a 16cm x 20cm x 20cm cube providing a thoroughly sufficient workspace to capture the full range of motion of the end effector.

Once implemented the two control methodologies function similarly having a user interface to select the desired position in task-space and monitor the current position of the end-effector. Figure 6a shows a screenshot of the IBVS user interface which is a feed from the webcam where the desired position can be selected with a mouse and the center of the ArUco marker can be monitored. Figure 6b shows an early implementation of EMTS with the marker taped onto the outside of the soft body, later moved internally. In EMTS the visual feed is no longer used, and the user interface is a 2D plane where the desired position can be selected with a mouse and the tracker position can be monitored. While the tracker provides a Cartesian pose in 6 DOF the movement is translated to a 2D task-space for the user to control. The 3DOF for orientation and the last degree of translation are ignored in the control methodology since the objective is to be able to make decisions in a 2D space.

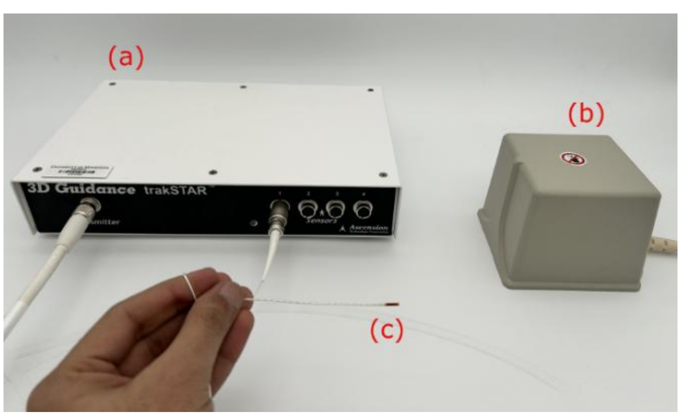

FIGURE 4: The electromagnetic (EM) tracking system components used for position feedback. (a) The Ascension trakSTAR desktop electronics unit. (b) The Mid-Range Transmitter (MRT) which generates the magnetic field for tracking. (c) The Model 130 6DOF sensor, which has a 1.5 mm outer diameter allowing it to be placed inside the soft robot's hollow center.

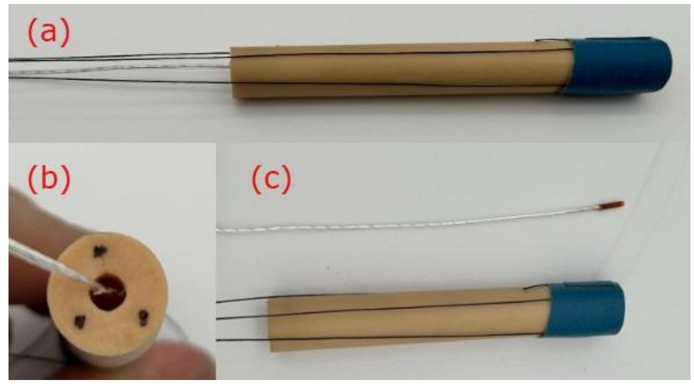

FIGURE 5: Electromagnetic tracking sensor with the soft robot. (a) Side view of the soft end effector housing the sensor. (b) Bottom view showing the central semi hollow chamber. (c) The Model 130 sensor positioned alongside the robot.

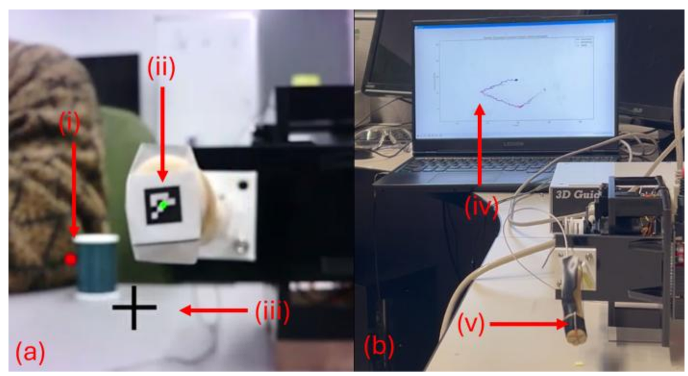

FIGURE 6: Control methodologies of the soft robot. (a) A screenshot from the IBVS user interface with (i) the desired position in pixel-space, (ii) the current position in pixel-space, (iii) the mouse cruiser for selecting desired position. (b) Implementation of EMTS showing (iv) a laptop displaying the user interface to control, (v) an initial implementation of EMTS with the marker taped to the outside of the soft body. Image resolution is due to images being taken from video recordings.

2.3 Control Methodology

The model-free control of the soft end effector is inspired by the control method of Wang et al. [6]. An initial Jacobian is estimated by having the motors run through a pre-determined short sequence, as shown in Figure 7 and tracking the position of the end effector using either the ArUco marker or electromagnetic tracker. The recorded end effector and known servo positions are used in a least squares method to initialize the Jacobian.

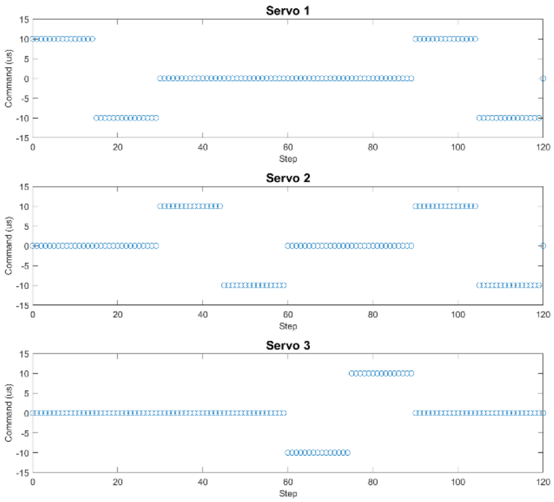

FIGURE 7: Pre-determined motor sequence to initialize the Jacobian. Each motor is commanded to change by fifteen 10us steps and then return to the initial position by fifteen 10us steps.

The kinematics of the robot can be represented as

$$\dot{\boldsymbol{p}} = \boldsymbol{J}\dot{\boldsymbol{q}} \tag{1}$$

where $\mathbf{J}$ is a 2x3 Jacobian and

$$\mathbf{p} = \begin{bmatrix} x \\ y \\ z \end{bmatrix} \tag{2}$$

is the end effector position in the task-space and

$$\mathbf{q} = \begin{bmatrix} q_1 \\ q_2 \\ q_3 \end{bmatrix} \tag{3}$$

is the position of each servo motor. Discretizing this system gives

$$\Delta\,\mathbf{p} = \mathbf{J}\Delta\,\mathbf{q} \tag{4}$$

Each time an actuator moves a new $\mathbf{q}$ and $\mathbf{p}$ matrix are formed which will be called $\mathbf{q}$(i) and $\mathbf{p}$(j) for **j = 0, 1, 2, 3, ...** giving

$$\Delta\mathbf{p}(j) = \mathbf{p}(j) - \mathbf{p}(j-1) \tag{5}$$

$$\Delta\mathbf{q}(j) = \mathbf{q}(j) - \mathbf{q}(j-1) \tag{6}$$

It is known that for an m x n matrix $\mathbf{A}$, an n x 1 vector $\mathbf{y}$, and an m x 1 vector $\mathbf{b}$

$$\mathbf{b} = \mathbf{Ay} \tag{7}$$

and the least squares method states that for known $\mathbf{A}$ and $\mathbf{b}$, the unknown $\mathbf{y}$ can be solved by using the Moore-Penrose pseudo-inverse

$$\mathbf{y} = \mathbf{A}^{+}\mathbf{b} \tag{8}$$

The servo and end effector positions can be used to form $\mathbf{A}$ and $\mathbf{b}$ such that,

$$\mathbf{A} = [\Delta\mathbf{q}(1)\;\; \Delta\mathbf{q}(2)\;\; \Delta\mathbf{q}(3)\; \cdots\; \Delta\mathbf{q}(\mathrm{j})] \tag{9}$$

$$\mathbf{b} = [\Delta\mathbf{p}(1)\;\; \Delta\mathbf{p}(2)\;\; \Delta\mathbf{p}(3)\; \cdots\; \Delta\mathbf{p}(\mathrm{j})] \tag{10}$$

We can then solve for $\mathbf{y}$ which will be the initial Jacobian $\mathbf{J_i}$. Once this initial Jacobian is found, it can be updated online while the end effector drives towards the final destination by continued tracking of the end effector position and repeated calculations using the least squares method.

The IBVS implementation captured video at 30FPS, and the last 10 sets of data points were used to determine the online Jacobian estimation. The EMTS implementation had an update rate of 80Hz, and the last 200 sets of data points were used to determine the online Jacobian estimation once the end effector was in motion. The number of data points along with either the video capture rate or the trakSTAR update rate can be tuned based on application to determine the optimal number of data points taking into account processing time and accuracy. The parameters used in this work were selected empirically based on observed performance in open-space trials and were not derived through formal optimization, further motivating application-specific tuning in future work.

To control the actuation of the motors based on desired position we use

$$\Delta\mathbf{q} = \mathbf{J}^{-1}\Delta\mathbf{p} \tag{11}$$

where the $\Delta\mathbf{p}$ is the desired change in end effector position to continue moving towards our final destination.

For this initial application, the desired trajectory was generated online by determining where the end effector was in relation to the desired final position and moving either 2 pixels (for IBVS) or 2mm (for EMTS) in XY position at each step towards the final position. This trajectory generation method was also used to determine the accuracy of the Jacobian estimation through inverse-mapping of task-space to joint-space, which generated a synergistic cable actuation sequence to reach the desired position. While this simple incremental movement approach effectively reduced the error between current and desired XY positions in task-space, it could be replaced by other methods such as pre-determined paths.

3. RESULTS AND DISCUSSION

As a result of the inverse mapping of the initial Jacobian from recorded task-space to joint-space was that although individual actuation was used to initialize the Jacobian, the inverse-map to obtain the same XY positions in task-space was a synergistic actuation of all three servos as seen in Figure 8.

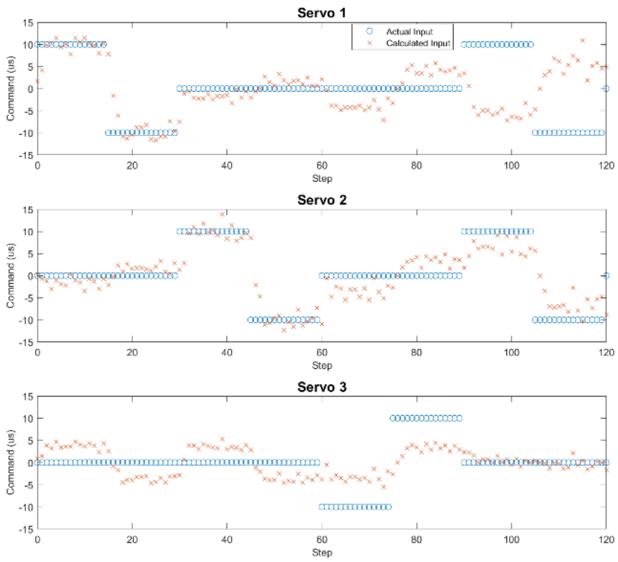

FIGURE 8: Inverse map of task-space to joint-space using the Initial Jacobian

Both control methodologies (IBVS and EMTS) were evaluated with both cable designs (internal and external cables), yielding successful outcomes across all four combinations. Given the similar performance observed across these configurations, presented are results from two representative pairings: the internal cable system controlled via IBVS and the external cable system controlled via EMTS.

The accuracy of the Jacobian estimation is best demonstrated by the plots in Figure 9 for the soft arm with cables running through its body, and Figure 10 for the soft arm with cables attached externally. The accuracy of the Jacobian estimation is demonstrated by the norm of the task-space error approaching zero between current position and commanded XY position. The internal cable soft robot system under IBVS control was able to successfully reduce the error between the current and commanded positions at each step of the control loop, shown in Figure 9. The external cable system controlled via EMTS was similarly successful as shown in Figure 10.

In both Figures 9 and 10 the error does not converge to zero which is a programmed behavior of the control loop. Once the error approaches zero it is necessary to prevent the Jacobian from becoming singular by continually moving the end position. This can be mitigated by discarding singular columns of data in the online estimation. This will keep the Jacobian updated to the current posture of the soft arm while keeping the end effector in the current position. In applications where another source is providing translation, such as the movement of a catheter through the pathways of the human body, being able to maintain position in XY while not reaching singularity will be necessary to ensure the correct path is maintained.

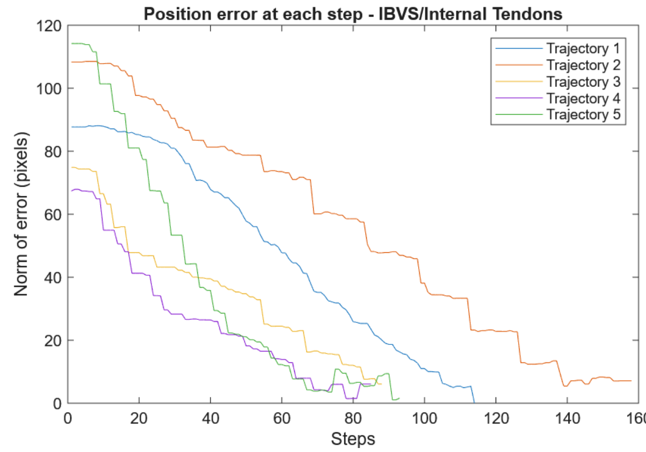

FIGURE 9: The reduction of the norm of the error in pixel-space between current position and commanded XY position for an internal cable system soft robot via controlled IBVS.

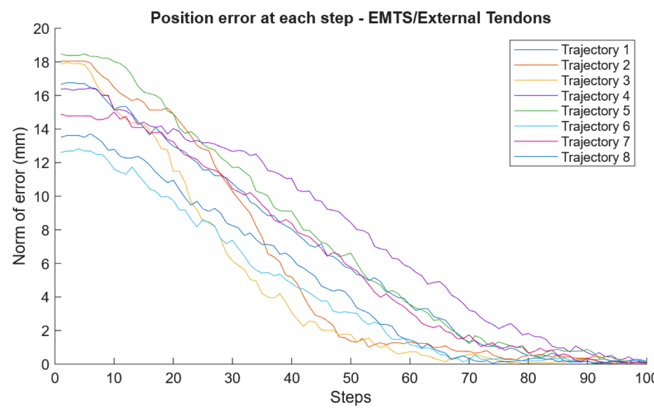

FIGURE 10: The reduction of the norm of the error in task-space between current position and commanded XY position for an external cable system controlled via EMTS.

Plots showing the target points with the commanded trajectory (labeled as *Trajectory*) and the actual followed path (labeled as *Path*) are shown for the internal cable system controlled via IBVS (Figure 11) and the external cable system controlled via EMTS (Figure 12). The jagged movement visible in Figure 11 reflects the 2-pixel step size used in IBVS, which produces coarser increments compared to the 2mm steps tracked in EMTS task-space, resulting in the smoother path seen in Figure 12. Especially noticeable in Figure 11 is that the paths appear to be saw-toothing, which is a result of the path calculation algorithm and can be improved in the future by implementing a more robust method of determining where the next step should be in task-space.

Both methods successfully reach the commanded XY positions, though the EMTS method follows a more direct path with less extraneous movement. Both figures also display the continuous tip movement around the target point to prevent the Jacobian from becoming singular. As this work represents an initial demonstration of online Jacobian estimation for a three-cable driven soft arm without a backbone, several limitations should be acknowledged. There are currently no benchmarks to compare this device to, and the

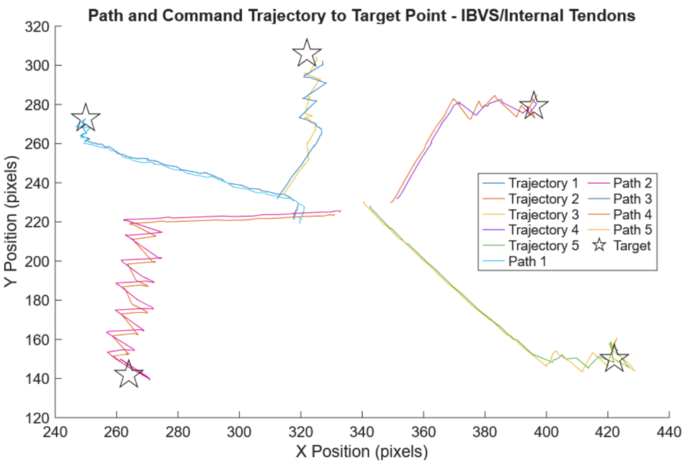

FIGURE 11: The commanded path (*Trajectory*) and the followed path (*Path*) in pixel space for the internal cable system controlled via IBVS to reach target points.

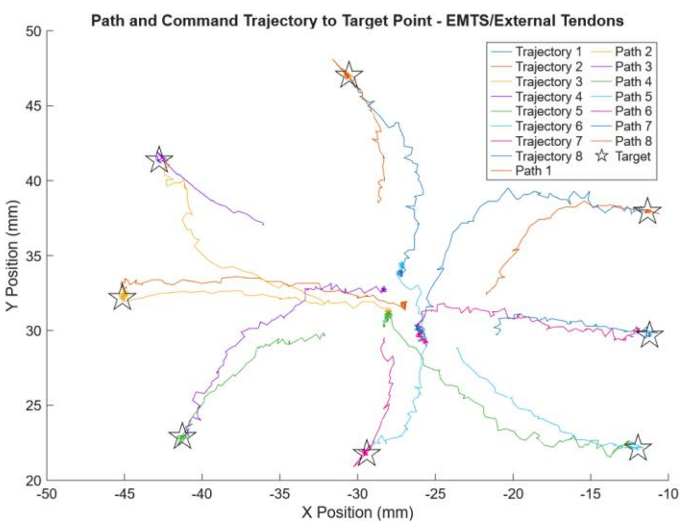

FIGURE 12: The commanded path (*Trajectory*) and the followed path (*Path*) in task-space for the internal cable system controlled via EMTS to reach target points.

current results reflect a limited number of trials rather than the hundreds of repeated experiments that would be required to fully characterize the statistical distribution of positioning accuracy and convergence behavior for both the IBVS and EMTS control schemes. The control was also validated only in unconstrained, open environments, leaving performance in the confined and tortuous pathways representative of human anatomy, the primary motivating application, yet to be assessed. Despite these limitations, the consistent reduction of task-space error to near zero across all four hardware and control methodology combinations provides preliminary evidence that motivates future large-scale statistical validation and testing in constrained environments.

4. CONCLUSION

Online Jacobian estimation using workspace exploration and local updating provides a model-free pathway to accurate end effector control in soft robotic systems that lack reliable closed-form analytical models. By eliminating the need for explicit kinematic modeling, this approach can be applied to other design and is independent of the actuation control scheme. The integration of electromagnetic tracking further extends the utility of the system to environments where optical occlusion renders vision-based feedback impractical, such as navigation within human anatomy. Future work includes trajectory tracking control in both open and constrained environments to further validate the robustness of the Jacobian estimation method and fully characterize the statistical distribution of positioning accuracy and convergence behavior.

ACKNOWLEDGEMENT

Caleb Fick from University of Minnesota, Minneapolis, MN fabricated the polyurethane soft end effector used in this work.

REFERENCES

[1] Webster III, R. J. and Jones, B. A., 2010, “Design and Kinematic Modeling of Constant Curvature Continuum Robots : A Review,” Int. J. Rob. Res., 29(13), pp. 1661–1683.
[2] Kormushev, P., Demiris, Y., and Caldwell, D. G., 2015, “Kinematic-free position control of a 2-DOF planar robot arm,” IEEE Int. Conf. Intell. Robot. Syst., doi:10.1109/IROS.2015.7354159.
[3] Li, G., Xu, S., Sun, L., and Liu, J., 2016, “Kinematic-free position control for a deformable manipulator,” Chinese Control Conf. CCC, 2016-Augus, pp. 10302–10307.
[4] Li, G., 2018, “Kinematic-Free Orientation Control for a Deformable Manipulator Based on the Geodesic in Rotation,” IEEE Robot. Autom. Lett., 3(3), pp. 2432–2438.
[5] Giorelli, M., Renda, F., Ferri, G., and Laschi, C., 2013, “A feedforward neural network learning the inverse kinetics of a soft cable-driven manipulator moving in three-dimensional space,” IEEE Int. Conf. Intell. Robot. Syst., doi:10.1109/IROS.2013.6697084.
[6] Wang, X., Denny, K.-h. L., Ziyang, K. C. F., Kui, D., Ge, W., Lee, F. S.-l., and Kwok, A. P. W. L. K.-w., 2018, “Experimental validation of robotassisted cardiovascular catheterization : model-based versus model-free control,” Int. J. Comput. Assist. Radiol. Surg., 13(6), pp. 797–804.
[7] Yip, M. C. and Camarillo, D. B., 2014, “Model-Less Feedback Control of Continuum Manipulators in Constrained Environments,” IEEE Trans. Robot., 30(2), pp. 352–364.
[8] Yip, M. and Camarillo, D., 2016, “Model-less Hybrid Position/Force control: A Minimalist Approach for Continuum Manipulators in Unknown, Constrained Environments,” IEEE Robot. Autom. Lett., 1(2), pp. 844– 851.
[9] Lee, K.-H., Fu, D. K., Leong, M. C., Chow, M., Fu, H.-C., Althoefer, K., Sze, K. Y., Yeung, C.-K., and Kwok, K.-W., 2017, “Nonparametric Online Learning Control for Soft Continuum Robot: An Enabling Technique for Effective Endoscopic Navigation,” Soft Robot., 4(4), p. Soro.2016.0065